arXiv:2205.00830v1 [hep-ph] 25 Apr 2022

The storage ring proton EDM experiment

Jim Alexander[7], Vassilis Anastassopoulos[36], Rick Baartman[28], Stefan Baeßler[39,22], Franco Bedeschi[19], Martin Berz[17], Michael Blaskiewicz[4], Themis Bowcock[33], Kevin Brown[4], Dmitry Budker[9,31], Sergey Burdin[33], Brendan C. Casey[8], Gianluigi Casse[34], Giovanni Cantatore[38], Timothy Chupp[34], Hooman Davoudiasl[4], Dmitri Denisov[4], Milind V. Diwan[4], George Fanourakis[20], Antonios Gardikiotis[30,36], Claudio Gatti[18], James Gooding[33], Renee Fatemi[32], Wolfram Fischer[4], Peter Graham[26], Frederick Gray[23], Selcuk Haciomeroglu[6], Georg H. Hoffstaetter[7], Haixin Huang[4], Marco Incagli[19], Hoyong Jeong[16], David Kaplan[13], Marin Karuza[37], David Kawall[29], On Kim[6], Ivan Koop[5], Valeri Lebedev[14,8], Jonathan Lee[27], Soohyung Lee[6], Alberto Lusiani[25,19], William J. Marciano[4], Marios Maroudas[36], Andrei Matlashov[6], Francois Meot[4], James P. Miller[3], William M. Morse[4], James Mott[3,8], Zhanibek Omarov[15,6], Cenap Ozben[11], SeongTae Park[6], Giovanni Maria Piacentino[35], Boris Podobedov[4], Matthew Poelker[12], Dinko Pocanic[39], Joe Price[33], Deepak Raparia[4], Surjeet Rajendran[13], Sergio Rescia[4], B. Lee Roberts[3], Yannis K. Semertzidis *[6,15], Alexander Silenko[14], Amarjit Soni[4], Edward Stephenson[10], Riad Suleiman[12], Michael Syphers[21], Pia Thoerngren[24], Volodya Tishchenko[4], Nicholaos Tsoupas[4], Spyros Tzamarias[1], Alessandro Variola[18], Graziano Venanzoni[19], Eva Vilella[33], Joost Vossebeld[33], Peter Winter[2], Eunil Won[16], Anatoli Zelenski[4], and Konstantin Zioutas[36]

[1] *Aristotle University of Thessaloniki, Thessaloniki, Greece*
[2] *Argonne National Laboratory, Lemont, Illinois, USA*
[3] *Boston University, Boston, Massachusetts, USA*
[4] *Brookhaven National Laboratory, Upton, New York, USA*
[5] *Budker Institute of Nuclear Physics, Novosibirsk, Russia*
[6] *Center for Axion and Precision Physics Research, Institute for Basic Science, Daejeon, Korea*
[7] *Cornell University, Ithaca, New York, USA*
[8] *Fermi National Accelerator Laboratory, Batavia, Illinois, USA*
[9] *Helmholtz-Institute Mainz, Johannes Gutenberg University, Mainz, Germany*
[10] *Indiana University, Bloomington, Indiana, USA*
[11] *Istanbul Technical University, Istanbul, Turkey*

[12] *JLAB, Newport News, Virginia, USA*
[13] *Johns Hopkins University, Baltimore, Maryland, USA*
[14] *Joint Institute for Nuclear Research, Dubna, Russia*
[15] *Physics Dept., KAIST, Daejeon, Korea*
[16] *Physics Dept., Korea University, Seoul, Korea*
[17] *Michigan State University, East Lansing, Michigan, USA*
[18] *National Institute for Nuclear Physics (INFN-Frascati), Rome, Italy*
[19] *National Institute for Nuclear Physics (INFN-Pisa), Pisa, Italy*
[20] *NCSR Demokritos Institute of Nuclear and Particle Physics, Athens, Greece*
[21] *Northern Illinois University, DeKalb, Illinois, USA*
[22] *Oak Ridge National Laboratory, Oak Ridge, TN, USA*
[23] *Regis University, Denver, Colorado, USA*
[24] *Royal Institute of Technology, Division of Nuclear Physics, Stockholm, Sweden*
[25] *Scuola Normale Superiore di Pisa, Pisa, Italy*
[26] *Stanford University, Stanford, California, USA*
[27] *Stony Brook University, Stony Brook, New York, USA*
[28] *TRIUMF, Vancouver, British Columbia, Canada*
[29] *UMass Amherst, Amherst, Massachusetts, USA*
[30] *Universität Hamburg, Hamburg, Germany*
[31] *University of California at Berkeley, Berkeley, California, USA*
[32] *University of Kentucky, Lexington, Kentucky, USA*
[33] *University of Liverpool, Liverpool, UK*
[34] *University of Michigan, Ann Arbor, Michigan, USA*
[35] *University of Molise, Campobasso, Italy*
[36] *University of Patras, Dept. of Physics, Patras-Rio, Greece*
[37] *University of Rijeka, Rijeka, Croatia*
[38] *University of Trieste and National Institute for Nuclear Physics (INFN-Trieste), Trieste, Italy*
[39] *University of Virginia, Charlottesville, Virginia, USA*

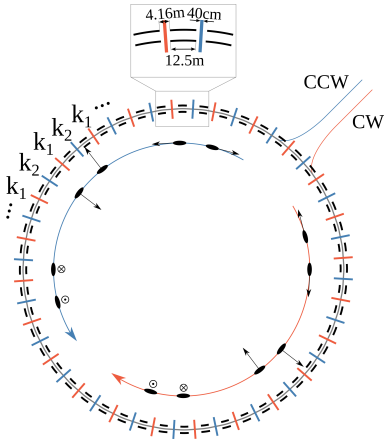
April 20, 2022

We describe a proposal to search for an intrinsic electric dipole moment (EDM) of the proton with a sensitivity of 10^{-29} $e \cdot$cm, based on the vertical rotation of the polarization of a

*Corresponding author, semertzidisy@gmail.com

stored proton beam. The New Physics reach is of order 1×10^3 TeV mass scale. Observation of the proton EDM provides the best probe of CP-violation in the Higgs sector, at a level of sensitivity that may be inaccessible to electron-EDM experiments. The improvement in the sensitivity to θ_{QCD}, a parameter crucial in axion and axion dark matter physics, is about three orders of magnitude.

One Page Summary of the Storage Ring Proton EDM Experiment



- Proton EDM sensitivity 10^{-29} $e \cdot$ cm.
- Improves the sensitivity to QCD CP-violation ($\theta_{\rm QCD}$) by three orders of magnitude, currently set by the neutron EDM experimental limits.
- New Physics reach is of order 1×10^3 TeV mass scale [1].
- Probes CP-violation in the Higgs sector with best sensitivity [2].
- Highly symmetric, magic momentum storage ring lattice in order to control systematics.
  - Proton magic momentum =0.7 GeV/c.
  - Proton polarimetry peak sensitivity at the magic momentum.
  - Optimal electric bending and magnetic focusing.
  - 2×10^{10} polarized protons per fill. One fill every twenty minutes.
  - Simultaneously stores clockwise (CW) and counterclockwise (CCW) bunches.
  - Simultaneously stores longitudinally polarized bunches with positive and negative helicities as well as radially polarized bunches.
  - 24-fold symmetric storage ring lattice.
  - Changes sign of the focusing/defocusing quadrupoles within 0.1% of ideal current setting per flip.
  - Keeps the vertical spin precession rate low when the beam planarity is within 0.1 mm over the whole circumference and the maximum split between the counter-rotating (CR) beams is < 0.01 mm.
  - Closed orbit automatically compensates spin precession from radial magnetic fields.
  - Circumference = 800 m with $E = 4.4$ MV/m, a conservative electric field strength.
- 3 – 5 years of construction and 2 – 3 years (for statistics collection) to first physics publication.
- Sensitive to dark matter, vector dark matter/dark energy (DM/DE) models [3, 4]. DM/DE signal proportional to $\beta = v/c$. Magic momentum pEDM ring $\beta = 0.6$.

- pEDM is highly complementary to atomic and molecular (AMO) EDM experiments [5]. AMO: many different effects, "sole source analysis", unknown cancellations [6].
- After proton EDM, can add magnetic bending for deuteron/^{3}He EDM measurements. Deuteron and ^{3}He EDM measurements complementary physics to proton EDM.

History

The proposed method has its origins in the measurements of the anomalous magnetic moment of the muon in the 1950-70s at CERN. The CERN I experiment [7] was limited by statistics. The sensitivity breakthrough was to go to a magnetic storage ring. The CERN II result was then limited by the systematics of knowing the magnetic field seen by the muons in the quadrupole magnet. The CERN III experiment [7, 8] used an ingenious method to overcome this. It was realized that an electric field at the so-called "magic" momentum does not influence the particle $(g-2)$ precession. Rather, the electric field precesses the momentum and the spin at exactly the same rate, so the difference is zero. The fact that all electric fields have this feature, opened up the possibility of using electric quadrupoles in the ring to focus the beam, while the magnetic field is kept uniform.

The precession rate of the longitudinal component of the spin in a storage ring with electric and magnetic fields is given by:

$$\frac{\mathrm{d}\boldsymbol{\beta}\cdot\boldsymbol{s}}{\mathrm{d}t} = -\frac{e}{m}\boldsymbol{s}_{\perp}\cdot\left[\left(\frac{g-2}{2}\right)\hat{\beta}\times\boldsymbol{B} + \left(\frac{g\beta}{2}-\frac{1}{\beta}\right)\frac{\boldsymbol{E}}{c}\right]. \tag{1}$$

The CERN III experiment used a bending magnetic field with electric quadrupoles for focusing at the "magic" momentum, given by $\beta^2 = 2/g$; see Equation (1) electric field term. The CERN III experiment and the BNL version of it, E821 [9], were limited by statistics, not systematics. The recent announcement of the $(g-2)$ experimental results [10] from Fermilab at 460 ppb has confirmed the BNL results, with similar statistical and smaller systematic errors. We believe that the FNAL E989 final results, at about 140 ppb, will have equal statistical and systematic errors. The storage ring/magic momentum breakthrough gained a factor of 2×10^3 in systematic error. BNL E821 set a "parasitic" limit on the EDM of the muon: $d_\mu < 1.9\times10^{-19}\ e\cdot\mathrm{cm}$ [11]. For FNAL E989, we expect this result to improve by up to two orders of magnitude. The statistical and systematic errors on the muon EDM will then be roughly equal. The dominant systematic error effect is due to radial magnetic fields.

For the pEDM experiment, we plan to use a storage ring at the proton magic momentum with electric bending and magnetic focusing, which gives a negligible radial magnetic field systematic effect — see below — while the dominant (main) systematic errors drop out with simultaneous clockwise and counter-clockwise storage. For both BNL E821 and FNAL E989, new systematic effects were discovered that were not in the original proposals. Several ways were applied to mitigate these small effects so they are not the limiting factors. For the pEDM experiment we can get 10^{11} polarized protons per fill from the BNL LINAC/Booster system, and we use symmetries to handle the systematics down to the level of sensitivity. We expect that at that level we perhaps will also discover new small systematics effects, as in the $(g-2)$ experiments.

Current searches for the EDM of fundamental particles have a large range of experimental sensitivity, as well as New Physics probing strength. Some of the strongest probes of New Physics come from the experimental limits of the electron (inferred indirectly from the atomic ThO EDM limit), the neutron and ^{199}Hg EDM limits [6, 12–17]. Their New Physics reach is the same within one order of magnitude of each other, while the proton EDM at $10^{-29}\ e\cdot\mathrm{cm}$ will bring a more than three orders of magnitude improved sensitivity over the current neutron limit. The current (indirect) experimental limit of the proton at $10^{-25}\ e\cdot\mathrm{cm}$ is derived from the ^{199}Hg atomic EDM limit. In the last three decades there has been a large effort to develop a stronger ultra-cold-neutron (UCN) source, e.g., see [6, 18–21], to enhance the probability for a higher sensitivity neutron EDM experiment beyond the few $10^{-28}\,e\cdot\mathrm{cm}$, the currently best experimental target for the neutron. Figure 1 shows the experimental limits of the neutron by publication year, the indirect proton EDM limits from the ^{199}Hg atomic EDM limit, and the projected sensitivity levels for the proton and deuteron using the storage ring EDM method. The ^{3}He sensitivity level is expected to be similar to that of the deuteron.

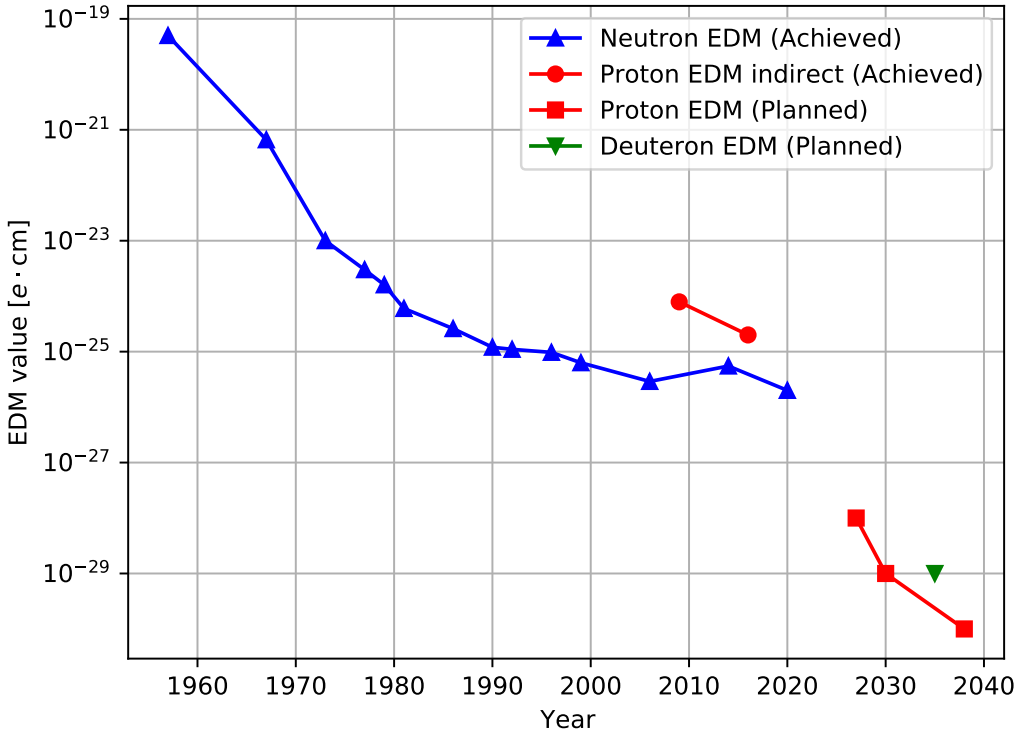


Figure 1: The neutron and proton (indirect) EDM limits by publication year are shown here. The storage ring EDM projected sensitivities for the proton and deuteron nuclei are also shown as a function of year. The ^{3}He nucleus storage ring EDM sensitivity is projected to be similar to that of the deuteron.

The storage ring EDM method

The concept of the storage ring EDM experiment is illustrated in Figure 2. There are three starting requirements: (1) The proton beam must be highly polarized in the ring plane. (2) The momentum of the beam must match the magic value of $p = 0.7007$ GeV/c, where the ring-plane spin precession is the same as the velocity precession, a condition called "frozen spin." (3) The polarization is initially along the axis of the beam velocity.

The electric field acts along the radial direction toward the center of the ring (E). It is perpendicular to the spin axis (p) and therefore perpendicular to the axis of the EDM. In this situation the spin will precess in the vertical plane as shown in Figure 2. The appearance of a vertical polarization component with time is the signal for a non-vanishing EDM. This signal is measured at the polarimeter where a sample of the beam is continuously brought to a carbon target. Elastic proton scattering is measured by two downstream detectors (shown in blue) [22, 23]. The rates depend on the polarization component p_y because it is connected to the *axial* vector created from the proton momenta $\vec{k}_{in} \times \vec{k}_{out}$. The sign of p_y flips between left and right as it follows the changing direction of $\vec{k}_{out}$. Thus, the asymmetry in the left-right rates, $(L-R)/(L+R) = p_y A$, is proportional to p_y and hence the magnitude of the EDM. The size of the effect at any given scattering angle also depends on the analyzing power A, a property of the scattering process. Having both left and right rates together reduces systematic errors.

A limited number of sensitive storage ring EDM experimental methods have been developed with various degrees of sensitivity and levels of systematic error, see Table 1 [1, 24]. Here we only address the method based on the hybrid-symmetric ring lattice, which has been studied extensively and shown to perform well, applying presently available technologies. The other methods, although promising, are outside the scope of this document, requiring additional studies and further technical developments.

The hybrid-symmetric ring method is built on the all-electric ring method, improving it in a number of critical ways that make it practical with present technology. It replaces electric focusing with alternating gradient magnetic focusing, still allowing simultaneous CW and CCW storage and eliminating the main systematic error source by design. A major improvement in this design is the enhanced ring-lattice symmetry, eliminating the next most-important systematic error source, that of the average vertical beam velocity within the bending sections [1].

Symmetries in the hybrid-symmetric ring with 10^{-29} $e \cdot$ cm sensitivity:

1. CW and CCW beam storage simultaneously.

2. Longitudinally polarized beams with both helicities.

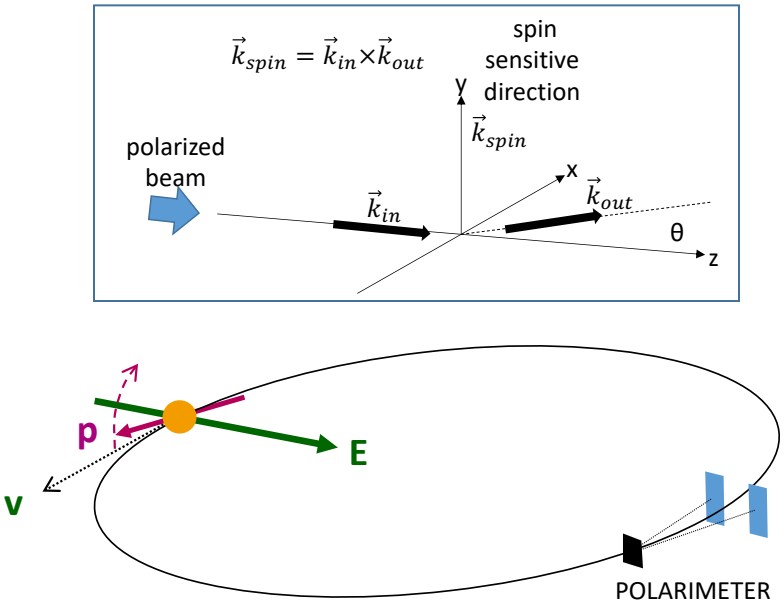


Figure 2: Diagram of the storage ring EDM concept, with the horizontal spin precession locked to the momentum precession rate ("frozen" spin). The radial electric field acts on the particle EDM for the duration of the storage time. Positive and negative helicity bunches are stored, as well as bunches with their polarization pointing in the radial direction, for systematic error cancellations. In addition, simultaneous clockwise and counterclockwise storage is used to cancel the main systematic errors. The ring circumference is about 800 m. The top inset shows the cross section geometry that is enhanced in parity-conserving Coulomb and nuclear scattering as the EDM signal increases over time.

Table 1: Storage ring electric dipole moment experiment options

Fields	Example	EDM signal term	Comments
Dipole magnetic field **B** (Parasitic).	Muon $(g-2)$ experiment.	Tilt of the spin precession plane. (Limited statistical sensitivity due to non-zero $(g-2)$ spin precession.)	Eventually limited by geometrical alignment. Requires consecutive CW and CCW injection to eliminate systematic errors.
Combination of electric and magnetic fields $(\mathbf{E},\mathbf{B})$ (Combined lattice).	Deuteron, ^{3}He, proton.	$\frac{\mathrm{d}\boldsymbol{s}}{\mathrm{d}t} \approx \boldsymbol{d}\times(\boldsymbol{v}\times\boldsymbol{B})$	High statistical sensitivity. Requires consecutive CW and CCW injection, with main fields flipping sign to eliminate systematic errors.
Radial Electric field (**E**) and Electric focusing (**E**) (All-electric lattice).	Proton.	$\frac{\mathrm{d}\boldsymbol{s}}{\mathrm{d}t} = \boldsymbol{d}\times\boldsymbol{E}$	Allows simultaneous CW and CCW storage. Requires demonstration of adequate sensitivity to radial $\boldsymbol{B}$-field systematic error source.
Radial Electric field (**E**) and Magnetic focusing (**B**) (Hybrid, symmetric lattice).	Proton.	$\frac{\mathrm{d}\boldsymbol{s}}{\mathrm{d}t} = \boldsymbol{d}\times\boldsymbol{E}$	Allows simultaneous CW and CCW storage. Only lattice to achieve direct cancellation of the main systematic error sources (its own "comagnetometer").

3. Radially polarized beams with both polarization directions.

4. Current flip of the magnetic quadrupoles.

5. Beam planarity to 0.1 mm and beam splitting of the counter-rotating (CR) beams to < 0.01 mm.

Strategy for building a high sensitivity hadronic EDM experiment

The storage ring EDM method for the proton and deuteron nuclei with frozen spin provides the potential for a high sensitivity of $10^{-29}\ e\cdot\mathrm{cm}$, as explained below in the "EDM Statistics" section. The reason for the high potential sensitivity is the availability of high-intensity, highly-polarized proton and deuteron beams with small phase-space emittance, since they are obtained from polarized ion sources, i.e., a primary source. Due to the negative value of the deuteron magnetic anomaly, the fields needed for the deuteron case are more complicated than for the proton and the uncertainties are thus larger [25]. The proton EDM ring, using the hybrid-symmetric ring lattice, has been studied extensively [1], see also [26, 27], and the conceptual design report (CDR) will be largely based on it. The cost of the experiment is similar to the muon $(g-2)$ cost of about \$100 M.

In preparing for the technical design report (TDR), we will assess the relevant concepts and techniques that have been studied so far [3, 4, 23, 28–42]. We will also:

1. Develop prototypes of polarimeters, with an emphasis on minimizing systematic errors and optimizing the statistical power of the method. Test the prototypes for high rates.

2. Study the optimum material, height, and shape of electric field plates with a field strength of 4.4 MV/m for 4 cm plate separation, in order to minimize the highest E—field value. Comment:

Small surface area E—field plates made of aluminum and coated with TiN have been developed and used at J-LAB; rather cheap and robust [43–45]. Need to expand this technology to large-area, about 20 cm high and 2 m long.

3. Construct a hydraulic level reference system (HLS) able to keep the ring planarity of the stored beam within 0.1 mm. A similar system developed at Fermilab [46, 47] would be adequate for the needs of the experiment.

4. Test a magnetometer capable of probing the separation of counter-rotating beams by 10 µm. SQUID-based magnetometers have demonstrated $10\,\mathrm{nm}/\sqrt{\mathrm{Hz}}$ in the lab [33] much better than needed; cheaper technologies are also available.

5. Develop a magnetic quadrupole prototype with emphasis on systematic error minimization when flipping the currents.

6. Design and construct a combined (hybrid) sextupole system including electric and magnetic fields.

7. Study the application of trim fields, both electric and magnetic, and develop prototypes of both.

8. Produce a detailed study of the RF-cavity, including a choice of the frequency and tunable range.

9. Construct a straight section equal to 1/48th of the ring and operate all elements together to discover any possible interferences.

A Highly Symmetric Lattice

A highly symmetric lattice is necessary to limit the EDM and dark matter/dark energy systematics, see [1, 3]. The 24-fold symmetric ring parameters are given in Table 2. The ring circumference is 800 m, with bending electric field 4.4 MV/m. This circumference is that of the BNL AGS tunnel, which would save tunnel construction costs. $E = 4.4\,\mathrm{MV/m}$ is conservative. A pEDM experiment at another location could have up to $E = 5\,\mathrm{MV/m}$ without R&D progress, see [43–45] and Figure 3, setting the scale of the required ring circumference.

Random misalignment of quadrupoles

Random misalignment of quadrupoles in both x, y directions leads to various systematic error sources. The systematic error sources directly caused by it are:

- Radial magnetic field.
- Vertical magnetic field.
- Vertical velocity.
- Geometric phase.

By randomly moving quadrupoles in the x, y direction by various σ amounts we can estimate the effect of such systematics. In addition, by repeating this procedure with multiple random seeds, we can eliminate the possibility of a "lucky configuration" — Figure 4.

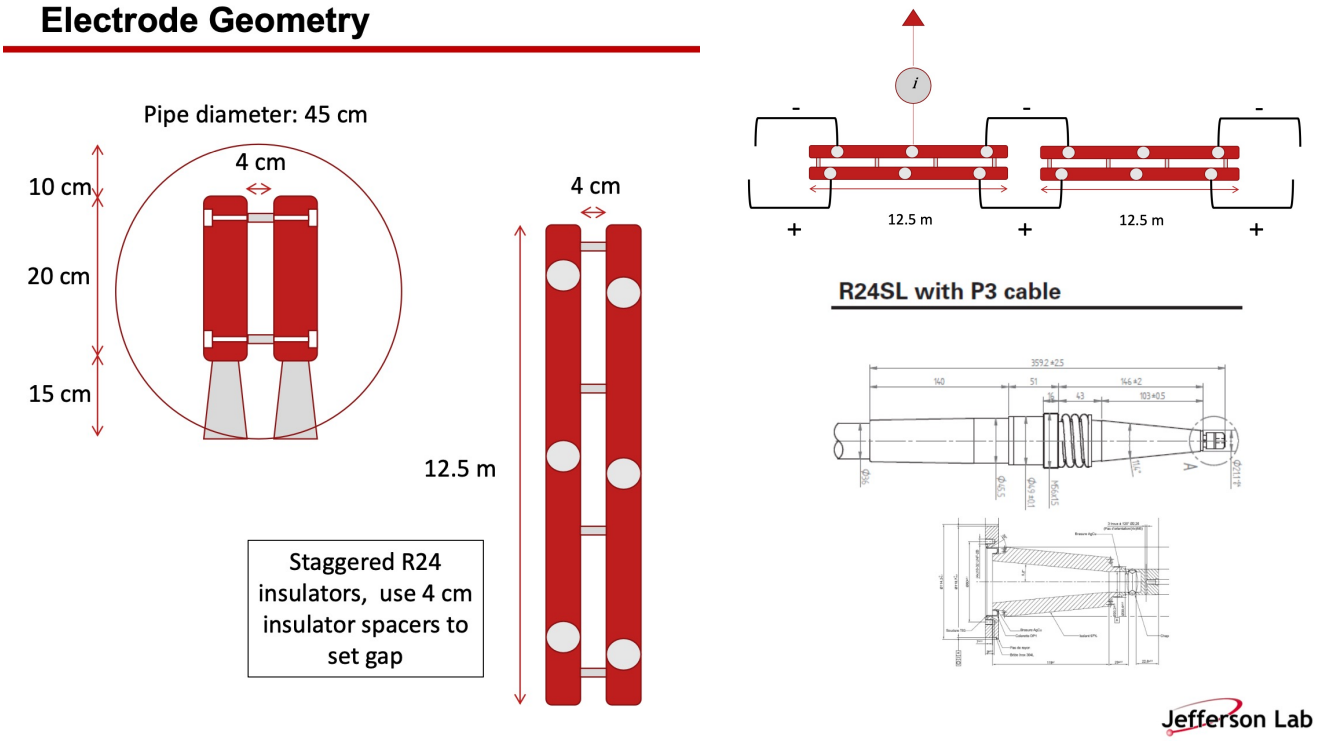


Figure 3: The cross-sectional and top views of the electric field plate design under consideration.

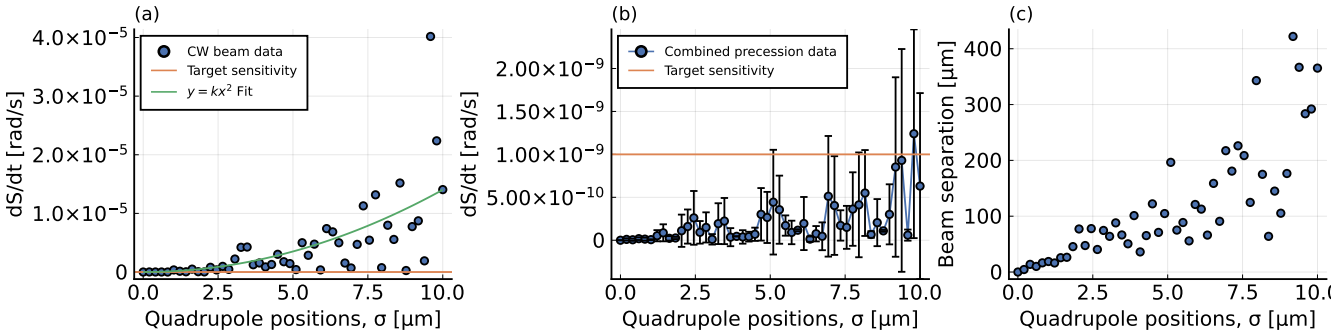


Figure 4: Total combined effect of the geometrical phase. (a) *Longitudinal clockwise.* Absolute value of vertical spin precession rates vs. σ quadrupole positions [μm] in both x and y directions (different random seeds were used for each point). (b) Same as (a) but complete data combination of CW and CCW with polarity switching is used. A large cancellation is achieved, allowing up to 10 µm random quadrupole misalignment. (c) Beam separation vs. quadrupole positions σ. As long as the beam separation can be measured to better than 100 µm, the geometrical phase should be under control.

Table 2: Ring and beam parameters for the hybrid-symmetric ring design. The beam planarity refers to the average vertical orbit of the counter-rotating (CR) beams with respect to gravity around the ring.

Quantity	Value
Bending Radius R_0	95.49 m
Number of periods	24
Electrode spacing	4 cm
Electrode height	20 cm
Deflector shape	cylindrical
Radial bending E-field	4.4 MV/m
Straight section length	4.16 m
Quadrupole length	0.4 m
Quadrupole strength	$\pm$0.21 T/m
Bending section length	12.5 m
Bending section circumference	600 m
Total circumference	800 m
Cyclotron frequency	224 kHz
Revolution time	4.46 µs
$\beta_x^{\max}$, $\beta_y^{\max}$	64.54 m, 77.39 m
Dispersion, $D_x^{\max}$	33.81 m
Tunes, Q_x, Q_y	2.699, 2.245
Slip factor, $\frac{dt}{t}/\frac{dp}{p}$	-0.253
Momentum acceptance, (dp/p)	5.2×10^{-4}
Horizontal acceptance [mm mrad]	4.8
RMS emittance [mm mrad], ϵ_x, ϵ_y	0.214, 0.250
RMS momentum spread	1.177×10^{-4}
Particles per bunch	1.17×10^8
RF voltage	1.89 kV
Harmonic number, h	80
Synchrotron tune, Q_s	3.81×10^{-3}
Bucket height, $\Delta p/p_{\text{bucket}}$	3.77×10^{-4}
Bucket length	10 m
RMS bunch length, σ_s	0.994 m
Beam planarity	0.1 mm
CR-beam splitting	0.01 mm

Table 3: "Magic" parameters for protons, values obtained from Ref. [48].

G	β	γ	p	KE
1.793	0.598	1.248	0.7 GeV/c	233 MeV

Spin Coherence Time

Spin Coherence Time (SCT), which is also recognized as in-plane polarization (IPP) lifetime, stands for the amount of time that the beam can stay longitudinally polarized. An SCT of around 10^3 s is required for the proton EDM experiment [49].

In order to demonstrate a large SCT, sextupoles with strengths $k^m_{1,2}$ are placed within (on top of) the magnetic quadrupoles. The sextupole fields are defined as,

$$B_x = 2k^m xy$$
$$B_y = k^m(x^2 - y^2).$$

Effectively, the entire storage ring is now covered with 24 sextupoles of strength k^m_1 and 24 sextupoles of strength k^m_2 (following the alternating pattern as the quadrupoles). In other words, the quadrupoles in addition to normal operation also act as sextupoles.

Although using correct magnetic sextupoles leads to a prolonged SCT, the same set of $k^m_{1,2}$ does not lead to a long SCT for both CR beams. A natural attempt would be to see how electrical sextupoles $k^e_{1,2}$ that are similar in strength affect the SCT, where the electric sextupoles are defined as,

$$E_x = -2k^e xy$$
$$E_y = k^e(x^2 - y^2).$$

If we assign magnetic sextupoles strength $k^m = k^m_1 = -k^m_2$ (alternating in sign like magnetic quadrupoles), and electric sextupoles $k^e = k^e_1 = k^e_2$ (same in sign like electrostatic deflectors), CW-CCW symmetry should be conserved in principle. By combining magnetic and electric sextupoles—"hybrid sextupoles"—the equivalence of CW-CCW is restored.

By using a realistic bunch structure (Figure 5), we see a large SCT improvement when using the hybrid set of sextupoles — Figure 6.

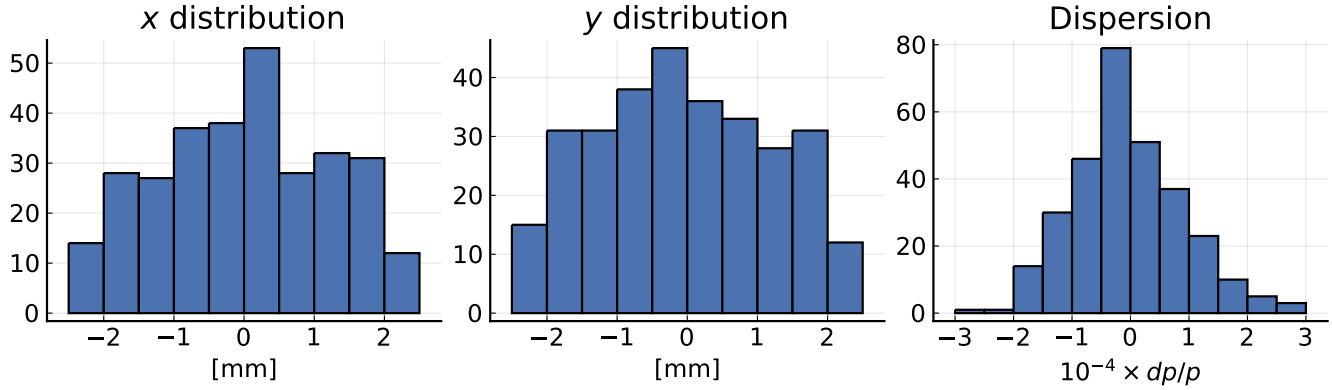


Figure 5: Bunch structure for both CR beams that is used to simulate the polarization lifetime, as shown in Figure 6.

Polarimetry

Tests with beams and polarimeters at several laboratories (BNL, KVI, COSY) have consistently demonstrated over more than a decade that the requirements of storage ring EDM search are within reach [23, 31, 32, 50–54]. Of particular importance, it has been shown that polarimeters based on forward elastic

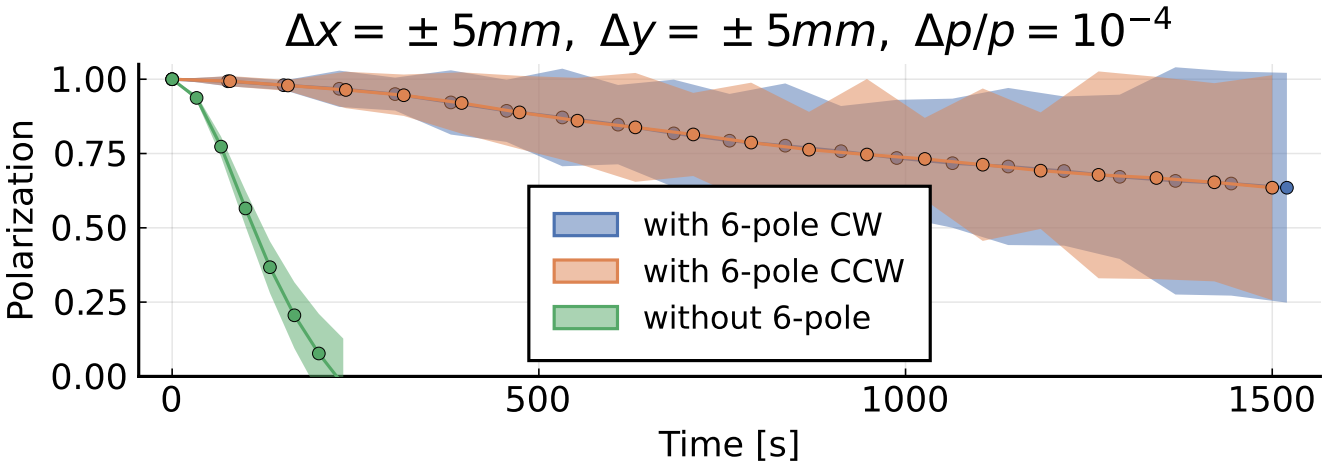


Figure 6: SCT is vastly prolonged when using the correct set of hybrid sextupoles.

scattering offer a way to calibrate and correct geometrical and counting rate systematic errors in real time. Sextupole field adjustments along with electron cooling yield long lifetimes for a ring-plane polarization whose direction may be controlled using polarimeter-based feedback. Given the extensive model-based studies demonstrating that ring designs using the symmetries described above can control EDM systematics at the 10^{-29} $e\cdot$cm level [1], the optimum path forward is to continue these developments on a full-scale hybrid, symmetric-lattice machine.

The features of the forward-angle elastic scattering polarimeter are listed below:

- Carbon target, observing elastic scattering between 5° and 15°. Target thickness: 2 cm to 4 cm. Angular distributions are shown in Figure 7 from Ref. [22].
- CW and CCW polarimeters share target in middle. Calibrate using vertical polarization.
- Detector: position sensitive ΔE, segmented calorimeter.
- Efficiency: $\sim 1\%$ of the particles removed from beam become part of the useful data stream.
- Analyzing power = 0.6, under Monte-Carlo (MC) estimation.
- Signal accumulation rate at 10^{-29} $e\cdot$cm is 10^{-9} rad/s.
- Full azimuthal coverage and forward/backward polarization allow first-order systematic error monitoring by using the four counting rates denoted by left/right detectors and forward/backward polarization. One combination of these rates is polarization insensitive while measuring a first-order driver of systematic errors. Corrections to the signal may be made to second-order in this driver in real time, which appears successful in correcting the signal at levels below 10^{-5} [23].

EDM Statistics

The statistical sensitivity of a single measurement, as exemplified by the neutron EDM case, is inversely proportional to the beam polarization, the analyzing power, the spin coherence time (SCT) and the square root of the number of detected events. The advantage of the storage ring method over using neutrons is

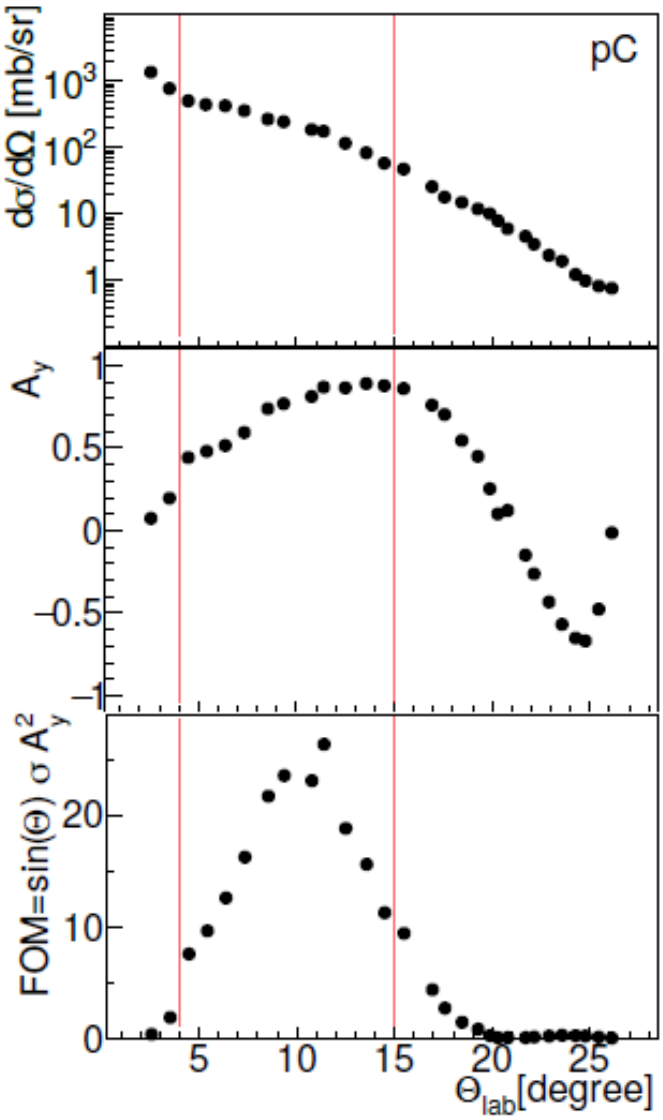


Figure 7: Angular distributions of p+C elastic scattering differential cross section, analyzing power, and modified figure of merit ($FOM = (\sin\theta)\sigma A_y^2$). The red lines show typical boundaries for data collection in a polarimeter.

that high-intensity, highly polarized beams with small values in the relevant phase-space parameters are readily available. As a consequence, it is possible to achieve long SCT with horizontally polarized beams, as was calculated analytically and demonstrated at COSY [31, 32].

Under optimized running conditions, where the beam storage duration is for half the SCT, the EDM statistical sensitivity of the method is given by [4],

$$\sigma_d = \frac{2.33\hbar}{P_0 A E \sqrt{k N_{cyc} T_{exp} \tau_p}}, \tag{2}$$

where P_0 (~ 0.8) is the horizontal beam polarization, A (~ 0.6) is the asymmetry, E ($3.3\,\mathrm{MV/m} = 4.4\,\mathrm{MV/m} \times 600\,\mathrm{m}/800\,\mathrm{m}$) is the average radial electric field integrated around the ring, k (1%) is the polarimeter detector efficiency, N_{cyc} ($\sim 2 \times 10^{10}$) is the stored particles per cycle, T_{exp} (1×10^8 s) is the total duration of the experiment and τ_p (2×10^3 s) is the in-plane (horizontal) beam polarization lifetime (equivalent to SCT). The SCT of 2×10^3 s, i.e., an optimum storage time of 10^3 s, is assumed here in order to achieve a statistical sensitivity at 10^{-29} $e \cdot$ cm level, while assuming the total experiment duration is 80 million seconds (in practice, corresponding to roughly five calendar years). Such a beam storage might require stochastic cooling due to IBS and beam-gas interactions. The estimated SCT of the beam itself (without stochastic cooling) as indicated by preliminary results with high-precision beam/spin-dynamics simulations is greater than 2×10^3 s, limited by the simulation speed.

Search for Axion-like Dark Matter in Storage Rings

Axion-like dark matter (DM) interacts with a nuclear EDM [55, 56]:

$$\mathcal{H} \propto g_{\mathrm{EDM}}\, a\, \hat{\mathbf{S}} \cdot \mathbf{E}. \tag{3}$$

This interaction induces an oscillating EDM, since a is a dynamic field: $d_n(t) = g_d a = d_0 \cos(m_a t)$, where m_a is the axion mass. Assuming that it makes up 100% of the local dark matter, the QCD axion induces an oscillating EDM of approximately 1×10^{-34} $e \cdot$ cm [57]. Axion-like particles (ALPs), which also may constitute the local DM, are less constrained than those of the QCD axion, motivating experimental searches even above the QCD axion band in the coupling parameter space.

Exploiting the dynamic nature of the nuclear EDM induced by the axion-like DM, proposed experimental approaches aim to enhance the signal using resonances, e.g. nuclear magnetic resonance in the CASPEr experiment [58–60] and vertical rotation of the polarization in the storage-ring axion-induced EDM experiment [4, 34]. The latter is conceptually similar to the storage-ring proton EDM experiment but it does not require the frozen-spin condition.

Figure 8 shows the ALP-EDM coupling parameter space, superimposed by experimentally excluded regions by (blue-filled) the neutron EDM measurement [61] and (orange-filled) the supernova energy loss [57]; theoretically plausible regions by (brown) the QCD axion band; (purple) ALP cogenesis where its lower and upper bounds correspond to $c_{aNN} = 1$ and 10 [62], respectively; (green) $Z_{\mathcal{N}}$ axion when it can account for the entire DM density [63, 64], and projected experimental sensitivity for (red-dashed) the storage-ring axion-induced EDM experiment including (magenta-dashed) parasitic measurement in the frozen-spin storage ring EDM experiment [4, 34]; and the CASPEr experiments [58–60]. For the storage-ring axion-induced EDM experiment, it assumes a spin coherence time of 10^4 seconds and one year of scientific data accumulation at each frequency, with 100 MV/m effective electric field ($E^* \equiv E - vB$) in the storage ring. There has also appeared a new constraint from the cold neutron-beam experiment at ILL[65]; it has not been included in Fig. 8 since it is not published yet.

The storage ring EDM method also allows us to look for ALP-nucleon coupling $\mathcal{H} \propto g_{aNN} \nabla a \cdot \hat{\mathbf{S}}$, as proposed in Ref. [3]. This interaction also induces a spin precession proportional to $g_{aNN} \cos(m_a t)$. A

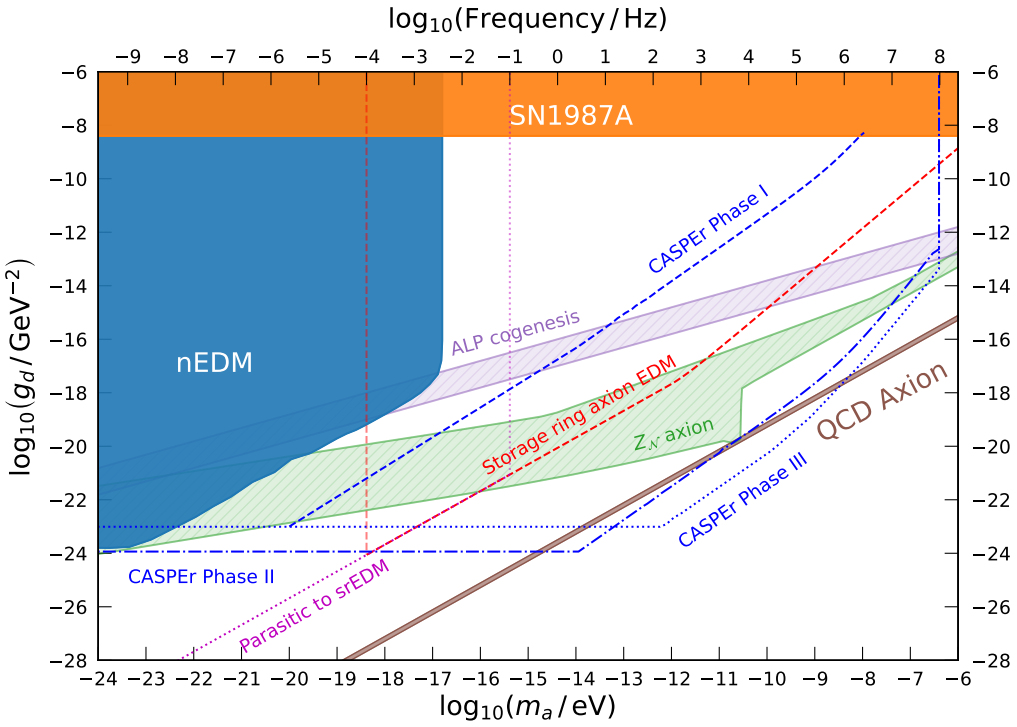


Figure 8: Parameter space for the ALP-EDM coupling strength g_d. Filled regions are excluded from (blue) the laboratory neutron EDM experiment [61] and (orange) astronomic constraints from the supernova cooling [57]. The other shaded regions are theoretically motivated regions from (brown) the QCD axion, (purple) the ALP cogenesis when the coupling constant c_{aNN} is between 1 and 10 [62] and (green) $Z_{\mathcal{N}}$ axion when it makes up the entire local dark matter density [63, 64]. Dashed lines indicate projected sensitivities proposed by (blue) the CASPEr experiment [58–60] and (red) the storage-ring axion-induced EDM experiment including (magenta) parasitic measurement in the frozen-spin storage ring EDM experiment [4, 34].

magnitude of the axion field gradient ∇a is boosted significantly when filled by a relativistic particle in a storage ring, providing a promising sensitivity on g_{aNN} with dedicated experimental configurations.

Conclusions

A storage ring proton EDM experiment offering unprecedented statistical sensitivity to the 10^{-29} $e \cdot$ cm level can be built based on present technology. The proposed method is based on the hybrid-symmetric ring lattice, the only lattice that eliminates the main EDM systematic error sources within the capacity of present technology. At the 10^{-29} $e \cdot$ cm level, this would be the best EDM experiment using one of the simplest hadrons. The facility would also permit studying the deuteron/^{3}He EDM with about an order of magnitude lower sensitivity. Finally, DM/DE experiments running in parasitic mode could probe previously unexplored parameter space.

References

[1]Z. Omarov, H. Davoudiasl, S. Hacıömeroğlu, V. Lebedev, W. M. Morse, Y. K. Semertzidis, A. J. Silenko, E. J. Stephenson, and R. Suleiman, "Comprehensive symmetric-hybrid ring design for a proton EDM experiment at below 10^{-29}e $\cdot$ cm", Phys. Rev. D **105**, 032001 (2022).

[2]W. Marciano, *Overview EDM theory*, `https://indico.fnal.gov/event/44782/timetable/?view=nicecompact`.

[3]P. W. Graham, S. Hacıömeroğlu, D. E. Kaplan, Z. Omarov, S. Rajendran, and Y. K. Semertzidis, "Storage ring probes of dark matter and dark energy", Phys. Rev. D **103**, 055010 (2021).

[4]O. Kim and Y. K. Semertzidis, "New method of probing an oscillating EDM induced by axionlike dark matter using an RF-Wien filter in storage rings", Phys. Rev. D **104**, 096006 (2021).

[5]N. Hutzler, *Developing New Directions in Fundamental Physics 2020*, `https://meetings.triumf.ca/event/89/contributions/2707`.

[6]T. E. Chupp, P. Fierlinger, M. J. Ramsey-Musolf, and J. T. Singh, "Electric dipole moments of atoms, molecules, nuclei, and particles", Rev. Mod. Phys. **91**, 015001 (2019).

[7]F. Combley, F. Farley, and E. Picasso, "The CERN muon $(g-2)$ experiments", Physics Reports **68**, 93–119 (1981).

[8]J. Bailey, K. Borer, F. Combley, H. Drumm, C. Eck, F. Farley, J. Field, W. Flegel, P. Hattersley, F. Krienen, et al., "Final report on the CERN muon storage ring including the anomalous magnetic moment and the electric dipole moment of the muon, and a direct test of relativistic time dilation", Nuclear Physics B **150**, 1–75 (1979).

[9]G. W. Bennett et al., "Final report of the E821 muon anomalous magnetic moment measurement at BNL", Physical Review D **73**, `10.1103/PhysRevD.73.072003` (2006-04-07).

[10]B. Abi et al. (Muon $g-2$ Collaboration), "Measurement of the Positive Muon Anomalous Magnetic Moment to 0.46 ppm", Phys. Rev. Lett. **126**, 141801 (2021).

[11]G. W. Bennett et al. (Muon (g-2) Collaboration), "Improved limit on the muon electric dipole moment", Phys. Rev. D **80**, 052008 (2009).

[12]C. Abel et al., "Measurement of the Permanent Electric Dipole Moment of the Neutron", Phys. Rev. Lett. **124**, 081803 (2020).

[13]C. A. Baker et al., "Improved Experimental Limit on the Electric Dipole Moment of the Neutron", Phys. Rev. Lett. **97**, 131801 (2006).

[14]V. Andreev et al., "Improved limit on the electric dipole moment of the electron", Nature **562**, Number: 7727 Publisher: Nature Publishing Group, 355–360 (2018-10).

[15]J. Baron et al., "Order of Magnitude Smaller Limit on the Electric Dipole Moment of the Electron", Science **343**, 269–272 (2014).

[16]B. Graner, Y. Chen, E. G. Lindahl, and B. R. Heckel, "Reduced Limit on the Permanent Electric Dipole Moment of ^{199}Hg", Phys. Rev. Lett. **116**, 161601 (2016).

[17]B. Graner, Y. Chen, E. G. Lindahl, and B. R. Heckel, "Erratum: Reduced Limit on the Permanent Electric Dipole Moment of ^{199}Hg [Phys. Rev. Lett. 116, 161601 (2016)]", Phys. Rev. Lett. **119**, 119901 (2017).

[18]F. Kuchler (and on behalf of TUCAN and HeXeEDM Collaborations), "Searches for Electric Dipole Moments—Overview of Status and New Experimental Efforts", Universe **5**, 1–11 (2019).

[19]R. Golub and J. Pendlebury, "Super-thermal sources of ultra-cold neutrons", Physics Letters A **53**, 133–135 (1975).

[20]R. Golub and J. Pendlebury, "The interaction of Ultra-Cold Neutrons (UCN) with liquid helium and a superthermal UCN source", Physics Letters A **62**, 337–339 (1977).

[21]Y. C. Shin, W. M. Snow, D. V. Baxter, C.-Y. Liu, D. Kim, Y. Kim, and Y. K. Semertzidis, "Compact ultracold neutron source concept for low-energy accelerator-driven neutron sources", Eur. Phys. J. Plus **136**, 882 (2021).

[22]H. O. Meyer et al., "Proton elastic scattering from ^{12}C at 250 MeV and energy dependent potentials between 200 and 300 MeV", Phys. Rev. C **37**, 544–548 (1988).

[23]N. Brantjes, V. Dzordzhadze, R. Gebel, F. Gonnella, F. Gray, D. Van Der Hoek, A. Imig, W. Kruithof, D. Lazarus, A. Lehrach, et al., "Correcting systematic errors in high-sensitivity deuteron polarization measurements", Nuclear Instruments and Methods in Physics Research Section A: Accelerators, Spectrometers, Detectors and Associated Equipment **664**, 49–64 (2012).

[24]F. J. M. Farley, K. Jungmann, J. P. Miller, W. M. Morse, Y. F. Orlov, B. L. Roberts, Y. K. Semertzidis, A. Silenko, and E. J. Stephenson, "New Method of Measuring Electric Dipole Moments in Storage Rings", Physical Review Letters **93**, 052001 (2004-07-27).

[25]V. Anastassopoulos et al., *AGS Proposal: Search for a permanent electric dipole moment of the deuteron nucleus at the* $10^{-29}e{\cdot}cm$ *level.* Access at: `https://www.bnl.gov/edm/files/pdf/deuteron_proposal_080423_final.pdf`, 2008-04.

[26]V. Anastassopoulos et al., "A storage ring experiment to detect a proton electric dipole moment", Review of Scientific Instruments **87**, 115116 (2016-11-29).

[27]S. Hacıömeroğlu and Y. K. Semertzidis, "Hybrid ring design in the storage-ring proton electric dipole moment experiment", Phys. Rev. Accel. Beams **22**, 034001 (2019).

[28]W. M. Morse, Y. F. Orlov, and Y. K. Semertzidis, "RF-Wien filter in an electric dipole moment storage ring: the 'partially frozen spin' effect", Physical Review Special Topics-Accelerators and Beams **16**, 114001 (2013).

[29]E. M. Metodiev, K. L. Huang, Y. K. Semertzidis, and W. M. Morse, "Fringe electric fields of flat and cylindrical deflectors in electrostatic charged particle storage rings", Physical Review Special Topics - Accelerators and Beams **17**, Publisher: American Physical Society, 074002 (2014-07-18).

[30]E. M. Metodiev et al., "Analytical benchmarks for precision particle tracking in electric and magnetic rings", Nuclear Instruments and Methods in Physics Research Section A: Accelerators, Spectrometers, Detectors and Associated Equipment **797**, 311–318 (2015-10).

[31]G. Guidoboni et al. (JEDI Collaboration), "How to Reach a Thousand-Second in-Plane Polarization Lifetime with 0.97−GeV/c Deuterons in a Storage Ring", Phys. Rev. Lett. **117**, 054801 (2016).

[32]N. Hempelmann et al. (JEDI Collaboration), "Phase Locking the Spin Precession in a Storage Ring", Phys. Rev. Lett. **119**, 014801 (2017).

[33]S. Hacıömeroğlu, D. Kawall, Y.-H. Lee, A. Matlashov, Z. Omarov, and Y. K. Semertzidis, "SQUID-based beam position monitor", The 39th International Conference on High Energy Physics, ICHEP2018 (2018).

[34]S. P. Chang, S. Hacıömeroğlu, O. Kim, S. Lee, S. Park, and Y. K. Semertzidis, "Axionlike dark matter search using the storage ring EDM method", Physical Review D **99**, 083002 (2019).

[35]A. J. Silenko, "Equation of spin motion in storage rings in the cylindrical coordinate system", Physical Review Special Topics-Accelerators and Beams **9**, 034003 (2006).

[36]A. J. Silenko, "Local Lorentz transformations and Thomas effect in general relativity", Phys. Rev. D **93**, 124050 (2016).

[37]Y. N. Obukhov, A. J. Silenko, and O. V. Teryaev, "Manifestations of the rotation and gravity of the Earth in high-energy physics experiments", Phys. Rev. D **94**, 044019 (2016).

[38]Y. N. Obukhov, A. J. Silenko, and O. V. Teryaev, "General treatment of quantum and classical spinning particles in external fields", Phys. Rev. D **96**, 105005 (2017).

[39]A. J. Silenko and O. V. Teryaev, "Equivalence principle and experimental tests of gravitational spin effects", Phys. Rev. D **76**, 061101 (2007).

[40]Y. Orlov, E. Flanagan, and Y. Semertzidis, "Spin rotation by Earth's gravitational field in a frozen-spin ring", Physics Letters A **376**, 2822–2829 (2012).

[41]A. László and Z. Zimborás, "Quantification of GR effects in muon ($g-2$), EDM and other spin precession experiments", Classical and Quantum Gravity **35**, 175003 (2018).

[42]S. Vergeles and N. Nikolaev, "Gravitational Effects in Electrostatic Storage Rings and the Search for the Electric Dipole Moments of Charged Particles", Journal of Experimental and Theoretical Physics **129**, 541–552 (2019).

[43]M. BastaniNejad et al., "Evaluation of niobium as candidate electrode material for dc high voltage photoelectron guns", Phys. Rev. ST Accel. Beams **15**, 083502 (2012).

[44]M. A. A. Mamun, A. A. Elmustafa, R. Taus, E. Forman, and M. Poelker, "TiN coated aluminum electrodes for DC high voltage electron guns", Journal of Vacuum Science & Technology A: Vacuum, Surfaces, and Films **33**, 031604 (2015).

[45]G. Palacios-Serrano, F. Hannon, C. Hernandez-Garcia, M. Poelker, and H. Baumgart, "Electrostatic design and conditioning of a triple point junction shield for a -200 kV DC high voltage photogun", Review of Scientific Instruments **89**, 104703 (2018).

[46]V. Shiltsev, "Review of observations of ground diffusion in space and in time and fractal model of ground motion", Phys. Rev. ST Accel. Beams **13**, 094801 (2010).

[47]V. Shiltsev, *Space-Time Diffusion of Ground and Its Fractal Nature*, Access at: `https://arxiv.org/pdf/0905.4194.pdf`, 2009-05.

[48]A. Mooser, S. Ulmer, K. Blaum, K. Franke, H. Kracke, C. Leiteritz, W. Quint, C. C. Rodegheri, C. Smorra, and J. Walz, "Direct high-precision measurement of the magnetic moment of the proton", Nature **509**, 596–599 (2014-05).

[49]V. Anastassopoulos et al., *A proposal to measure the proton electric dipole moment with* $10^{-29}e{\cdot}cm$ *sensitivity, by the Storage ring EDM collaboration*, Oct. 2011.

[50]N. Hempelmann et al. (JEDI Collaboration), "Phase measurement for driven spin oscillations in a storage ring", Phys. Rev. Accel. Beams **21**, 042002 (2018).

[51]G. Guidoboni et al. (JEDI Collaboration), "Connection between zero chromaticity and long in-plane polarization lifetime in a magnetic storage ring", Phys. Rev. Accel. Beams **21**, 024201 (2018).

[52]A. Saleev et al. (JEDI collaboration), "Spin tune mapping as a novel tool to probe the spin dynamics in storage rings", Phys. Rev. Accel. Beams **20**, 072801 (2017).

[53]D. Eversmann et al. (JEDI collaboration), "New Method for a Continuous Determination of the Spin Tune in Storage Rings and Implications for Precision Experiments", Phys. Rev. Lett. **115**, 094801 (2015).

[54]Z. Bagdasarian et al., "Measuring the polarization of a rapidly precessing deuteron beam", Phys. Rev. ST Accel. Beams **17**, 052803 (2014).

[55]F. Chadha-Day, J. Ellis, and D. J. E. Marsh, "Axion dark matter: what is it and why now?", Science Advances **8**, eabj3618 (2022).

[56]Y. K. Semertzidis and S. Youn, "Axion dark matter: How to see it?", Science Advances **8**, eabm9928 (2022).

[57]P. W. Graham and S. Rajendran, "New observables for direct detection of axion dark matter", Phys. Rev. D **88**, 035023 (2013).

[58]D. Budker, P. W. Graham, M. Ledbetter, S. Rajendran, and A. O. Sushkov, "Proposal for a Cosmic Axion Spin Precession Experiment (CASPEr)", Phys. Rev. X **4**, 021030 (2014).

[59]D. F. J. Kimball et al., *Overview of the Cosmic Axion Spin Precession Experiment (CASPEr)*, Access at: `https://arxiv.org/pdf/1711.08999.pdf`, 2017.

[60]D. Aybas et al., "Search for Axionlike Dark Matter Using Solid-State Nuclear Magnetic Resonance", Phys. Rev. Lett. **126**, 141802 (2021).

[61]C. Abel et al., "Search for Axionlike Dark Matter through Nuclear Spin Precession in Electric and Magnetic Fields", Phys. Rev. X **7**, 041034 (2017).

[62]R. T. Co, L. J. Hall, and K. Harigaya, "Predictions for axion couplings from ALP cogenesis", Journal of High Energy Physics **2021**, 172 (2021).

[63]L. D. Luzio, B. Gavela, P. Quilez, and A. Ringwald, "Dark matter from an even lighter QCD axion: trapped misalignment", Journal of Cosmology and Astroparticle Physics **2021**, 001 (2021).

[64]L. Di Luzio, B. Gavela, P. Quilez, and A. Ringwald, "An even lighter QCD axion", Journal of High Energy Physics **2021**, 184 (2021).

[65]I. Schulthess et al., *New Limit on Axion-Dark-Matter using Cold Neutrons*, Access at: `https://arxiv.org/pdf/2204.01454.pdf`, 2022.